Food Chemistry 433 (2024) 137274

Contents lists available at ScienceDirect

Food Chemistry

journal homepage: www.elsevier.com/locate/foodchem

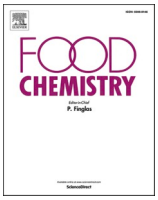

Antioxidant efficiency and oxidizability of mayonnaise by oximetry and isothermal calorimetry

Rajat Suhag [a], Giovanna Ferrentino [a], Ksenia Morozova [a], Daniele Zatelli [b], Matteo Scampicchio [a,*], Riccardo Amorati [c]

[a] Faculty of Agricultural, Environmental and Food Sciences, Free University of Bolzano, Piazza Università, 1, Bolzano 39100, Italy
[b] Research and Development, VOG Products, Bolzano, Italy
[c] Department of Chemistry "G. Ciamician", University of Bologna, Via S. Giacomo 11, Bologna I-40126, Italy

ARTICLE INFO

Keywords:
Induction time
Fatty acids
Antioxidant activity
Lipid oxidation
Oxidation rate

ABSTRACT

This study aimed to introduce a new method based on isothermal calorimetry (IC) for measuring the autoxidation rate in mayonnaise samples. Mayonnaise samples were prepared by homogenizing an aqueous phase, consisting of vinegar and egg yolk, with various oil phases, including sunflower, corn, extra virgin olive, grape seed, and apple seed oils at 60 °C. The rate of free radical formation (R_i) was controlled by adding AIBN (R_i = 4.4 $\pm 0.1 \times 10^{-9}$ M/s). The autoxidation rate determined by IC was highly correlated with the one measured using the oxygen uptake method (R^2 = 0.99). The IC method accurately indicated the antioxidant capacity and rates of both inhibited and uninhibited periods, together with the oxidizability of mayonnaise samples. The mayonnaise made with extra virgin olive oil exhibited the lowest oxidizability, while sunflower oil showed maximum antioxidant efficiency. A significant advantage of the IC method was its ability to simultaneously measure up to 24 samples with minimal effort.

1. Introduction

Lipid autoxidation is a significant concern for the food industry because it results in nutrient loss, forms potentially toxic compounds, and produces "off" odours (Berton-Carabin et al., 2014). Unsaturated lipids are especially prone to autoxidation, highlighting the need for antioxidants to effectively slow the oxidation process (Wang et al., 2023). In food emulsions, such as mayonnaise, the large surface area of oil droplets, when compared to bulk oils, amplifies the lipids' susceptibility to oxidation (ten Klooster et al., 2023; Schröder et al., 2019; Villeneuve et al., 2023). Consequently, ongoing research is essential to investigate and develop natural and safe antioxidants that can effectively inhibit lipid autoxidation processes, boost food product stability, and extend shelf-life (Carocho et al., 2018).

While it is crucial to study lipid peroxidation under realistic conditions, the current methods for monitoring oxidation kinetics have limitations. Methods, such as measuring hydroperoxides (early oxidation products) or volatile aldehydes (late oxidation products) provide valuable kinetic insights but are discontinuous, requiring repeated sample withdrawals (Culler et al., 2022; Frankel et al., 1989; Koelsch et al., 1991). Conversely, methods like Rancimat and Oxitest provide continuous monitoring but are constrained to high-temperatures, approximately 90 – 160 °C (Tinello et al., 2018).

The kinetic mechanism of lipid autoxidation encompasses the concurrent processes of initiation, propagation, and termination within a radical chain mechanism (Edwin N Frankel, 2012). For an accurate quantitative kinetic analysis of this mechanism, controlling the initiation's rate is crucial. This control is typically achieved using initiators like AIBN (azo-bis-isobutyronitrile), a lipid soluble free radical generator. AIBN thermally decomposes at a known and constant rate, generating a flux of free radicals (Sicari et al., 2018). Such controlled mechanism facilitates the evaluation of antioxidants' efficiency in inhibiting peroxidation, especially considering the correlation of the propagation reaction with the content and nature of unsaturated fatty acids.

Oximetry, a versatile and non-invasive technique, is commonly used to study lipid peroxidation through the oxygen uptake method (Amorati & Valgimigli, 2015; Amorati & Valgimigli, 2018; Baschieri & Amorati, 2021). On the other hand, isothermal calorimetry uses heat flow sensors to measure the heat generated during both inhibited and uninhibited

* Corresponding author.
E-mail address: Matteo.scampicchio@unibz.it (M. Scampicchio).

https://doi.org/10.1016/j.foodchem.2023.137274
Received 3 April 2023; Received in revised form 21 August 2023; Accepted 22 August 2023
Available online 29 August 2023

periods of lipid peroxidation. This method also allows for the simultaneous analysis of several samples and maintains outstanding thermal stability over prolonged time.

To validate the suitability of isothermal calorimetry in assessing the oxidative stability of mayonnaise, both isothermal calorimetry and oximetry were applied to different mayonnaise formulations. These were prepared by homogenizing a consistent aqueous phase (consisting of vinegar and egg yolk) with various oil phases, including sunflower, corn, extra virgin olive, grape seed, and apple seed oils. Assays like DPPH (2,2-diphenyl-1-picrylhydrazyl) and ORAC (oxygen radical absorbance capacity) provide information about the radical-scavenging capacity of antioxidants, which is crucial for assessing their effectiveness in preventing lipid oxidation. The Folin-Ciocalteu method quantifies the oil's total polyphenol content, which is a recognized attribute for characterizing their antioxidant properties. Measuring the polyphenol content and its correlation with sample oxidative stability elucidates the polyphenols' role in the mayonnaise's antioxidant capacity.

This study introduces a novel isothermal calorimetry (IC) method for continuous monitoring of peroxidation rates at 60 °C and evaluates its reliability compared to oximetry. We investigate the peroxidation of mayonnaise samples made with different seed oils, each with unique levels of polyunsaturated lipids and antioxidants. Through IC analysis, the study aims to gain valuable kinetic insights into the relationship between oil composition, antioxidant activity, and oxidation rate. Thus, this research focuses on the antioxidant efficiency and oxidizability of mayonnaise samples by comparing two methods: oximetry and isothermal calorimetry.

By examining the oxidizability of different oils and their interaction with antioxidants in mayonnaise, this study introduces IC as a novel approach to study the oxidative stability and antioxidant activity of emulsion systems. In alignment with the research objectives outlined earlier, we hypothesized that IC can identify seed oils rich in polyunsaturated lipids that exhibit higher oxidizability in mayonnaise samples. Furthermore, the method is expected to predict those antioxidant-rich samples that exhibit significant chain-breaking capacity, effectively inhibiting lipid peroxidation in emulsion systems. Overall, the application of IC to measure peroxidation rates in realistic food matrices, like mayonnaise, can provide useful insights for the food industry in the development of effective antioxidant strategies to preserve food emulsions.

2. Materials and methods

2.1. Materials

Commercially available oils included (1) sunflower, (2) corn, (3) extra virgin olive, (4) apple seed and (5) grapeseed oil. They were purchased from Sulu Organics, Illinois, USA. Raw eggs and white wine vinegar were purchased from a local market in Bolzano, Italy. Sodium azide, azobisisobutyronitrile (AIBN), Folin–Ciocalteu's reagent, 1,1-diphenyl-2 picrylhydrazyl (DPPH), gallic acid, 2,2′-Azobis(2-amidinopropane) dihydrochloride (AAPH), fatty acid methyl esters (Supelco FAMEs Mix GLC-30) and trolox were bought from Sigma Aldrich Chemical Co. (Italy). All solvents and reagents were of analytical grade.

2.2. Mayonnaise preparation

Mayonnaise samples were prepared by mixing oil (80%), egg yolk (10%), and vinegar (10%). Sodium azide (0.05% w/w) was incorporated as microbial inhibitor. The lipid soluble radical initiator AIBN was integrated into the oil phase to achieve a final concentration of 25 mM. Ingredients were combined in a glass beaker placed in an ice bath. A high shear homogenizer (IKA, T-25 digital ULTRA-TURRAX®, Germany) was utilized for mixing. Initially, all ingredients, excluding the oil, were mixed for 1 min at 15,000 rpm. Then, oil was added dropwise. After 5 min, the speed was adjusted to 20,000 rpm while continuing to add the oil dropwise. The final mayonnaise sample was obtained after 15 min of continuous blending. Samples were labelled based on the oil type: MSO, MCO, MEVOO, MGO and MAO, respectively, for sunflower, corn, extra virgin olive, grapeseed, and apple seed oils. Samples were stored at 4 °C for subsequent analysis. Particle size determination of mayonnaise samples was conducted using the method described by Yildirim et al., (2016) with a Mastersizer 3000 (Malvern, United Kingdom). The pH determination of the samples is provided in Supplementary Table S1.

2.3. Oxidative stability by isothermal calorimetry

The oxidative stability of mayonnaise samples was determined with an isothermal calorimeter (Thermal Activity Monitor, Model 421 TAM III, TA Instruments). The experiment procedure followed that reported by Valoppi et al., (2020). Briefly, the calorimeter was preliminarily conditioned at 60 °C. Then, each channel of the calorimeter was calibrated with a gain calibration process with electric impulses, as recommended by the manufacturer. After calibration, the mayonnaise samples (200±5 mg) were filled into hermetically sealed glass ampoules (4.0 cm^3). Then, the ampoules were positioned inside the calorimeter and kept in an equilibration position for 15 min (that is a negligible time respect the duration of the experiment). This step allowed to equilibrate the temperature of the sample with that of the calorimeter (60 °C). Then, the ampoule was moved to the measurement position and the recording of the heat flow signal over time started.

2.4. Oximetry

The oxygen concentration inside the glass ampoules was monitored using an oxygen meter (Fibox 4, PreSens GmbH, Germany). The meter was equipped with a 5 mm luminescence oxygen sensor (Pst3), which was secured to the inner surface of the glass ampoules. The measurements emulated the experimental conditions of the isothermal calorimetry method. Thus, a mayonnaise sample (200±5 mg) was placed in a sealed glass ampoule and stored in a Peltier incubator (IPP30 Plus, Memmert, Germany) at 60±0.5 °C. The accuracy of the oxygen sensors was tested with various air and nitrogen mixtures prior to analyzing the samples. Measurements were recorded every 5 min.

2.5. Fatty acids profiling of oils using GC-FID

Fatty acid profile was determined by a gas chromatograph (Thermo Scientific TRACE 1300, Italy) coupled with a flame ionization detector (GC-FID) and fused silica capillary column (TG-Polar, Thermo Scientific, length (60 m), internal diameter (0.25 mm) and film thickness of 0.2 μm) as described by Ferrentino et al., (2020). Hydrogen gas, at a flow rate of 3 mL min^{-1} was used as a carrier gas. About 100 μL of oil sample and 8 mL *n*-hexane were mixed and vortexed, 300 μL of 2 M methanolic KOH was added and again vortexed, after 5 min the upper layer was transferred to glass vials for further analysis. Injector and detector temperatures were maintained at 260 °C and 300 °C, respectively. The column temperature was maintained at 50 °C for a min and then raised to 175 °C (heating rate = 5 °C min^{-1}), and ultimately raised to 250 °C (heating rate = 1 °C min^{-1}. FAMEs were detected by comparing the retention durations and quantified using the calibration curves prepared with analytical standards.

The concentration (mol/L) of oxidizable substrate $[RH]_0$ in mayonnaise samples was calculated with Eq. (1).

$$[RH]_0 = \sum_i \frac{[FA_i]_0}{MW_i} \times \rho \times 0.8 \quad (1)$$

Where $[FA_i]_0$ is the initial concentration of each fatty acid (g/kg) determined by GC-FID (Supplementary Table S2), MW_i (g/mol) is their molecular weight, ρ is the oil density (0.92 kg/L) and 0.8 is the mass

fraction of the oil in mayonnaise samples.

2.6. Preparation of ethanolic extracts

Oil samples (1 mL) were placed into to centrifuge tubes, followed by the addition of 9 mL of ethanol (100%). These tubes were then vortexed for 1 min and sonicated at 25 °C for 5 min. This procedure was repeated thrice. The oil and ethanol mixture was allowed to stand at room temperature for 1 h, then centrifuged at 10,000 rpm and 10 °C for 10 min. The upper layer was carefully transferred to a new tube. The oil residues underwent re-extraction with ethanol three times. Extracted portions from all steps were combined, and residual solvent from the ethanolic extracts was evaporated using a rotary vapor evaporator (Hei-VAP, Heidolph, Germany) under reduced pressure. After evaporation, 9 mL of ethanol was added to obtain the final extract.

2.7. DPPH assay

Antioxidant activity in the ethanolic extracts of oils was assessed using the DPPH test, as defined by Brand-Williams et al., (1995), with some modifications. About 8 mg DPPH was dissolved in ethanol (200 mL) to prepare the DPPH reagent. For the assay, 1900 μL of this reagent was combined with 100 μL of ethanolic extract. This mixture was then stored in dark at room temperature for 1 h. Absorbance readings were taken at 515 nm using a UV–Vis spectrophotometer (Cary 100 Series, Agilent technologies, Italy). Antioxidant activity was determined using Trolox standard calibration curve.

2.8. Total phenolic content

Total phenolic content of ethanolic extracts of oils was determined as described by Valoppi et al., (2020). In a 2 mL cuvette, 40 μL extract, 1200 μL distilled water, 300 μL sodium carbonate solution (20% in distilled water), and 100 μL Folin-Ciocalteau reagent were added and kept in dark at room temperature for 2 h. Then, absorbance readings were taken at 765 nm with a UV–Vis spectrophotometer (Cary 100 Series, Agilent technologies, Italy). A standard calibration curve of gallic acid was used to calculate total phenolic content.

2.9. Oxygen radical absorbance capacity (ORAC)

The ORAC assay followed the method of Ou et al., (2001) with some modifications. Measurements utilized a 96 well black-walled plate, each with a 200 μL final volume. All solutions were prepared in a phosphate buffer (pH 7.0, 75 mM). Each well received 50 μL of a fluorescein working solution (800 nM), 50 μL of either the diluted extract or a Trolox solution with concentrations ranging from 0 to 100 μM. Once prepared, the plate was positioned inside a microplate reader (Infinite M nano^{+}, Tecan, Switzerland), configured to excitation and emission wavelengths of 480 and 535 nm, respectively. The plate incubated at 37 °C for 30 min. Before readings, 100 μL of AAPH (100 mM) was introduced to each well using a multi-pipette. Absorbance was then read every minute over a 120-min period to reach a relative fluorescence intensity of 5%. Results derived from the area under the curve (AUC) differences between the blank and a given sample.

2.10. Lipid peroxidation kinetic model

Lipid peroxidation follows a radical chain mechanism comprising three main steps: initiation, propagation, and termination reactions. The initiation rate is typically controlled using AIBN (azo-bis-isobutyronitrile), a lipid soluble free radical generator. This compound thermally decomposes at a known and constant rate, generating a flux of tertiary radicals (Eq. (2)):

$$\text{Initiation}: \ \text{AIBN} \xrightarrow{k_i} 2\text{R}\bullet + \text{N}_2 \tag{2}$$

These radicals quickly react with oxygen ($k_0 \approx 10^9\ \text{M}^{-1}\text{s}^{-1}$) leading to peroxyl radicals (Domínguez et al., 2019) (Eq. (3)):

$$(very\ fast) R\bullet + O_2 \xrightarrow{k_o} ROO\bullet \tag{3}$$

Peroxyl radicals then react with unsaturated lipids by hydrogen transfer to form hydroperoxides. These reactions are referred to as "propagation" (Eq. (4)) because each reaction generates another radical, keeping the "chain" alive:

$$Propagation: ROO\bullet + RH \xrightarrow{k_p} ROOH + R\bullet \tag{4}$$

Finally, two peroxyl radicals can interact with each other to form non radical products (NRP) through a "termination" reaction (Eq. (5)):

$$Termination: 2ROO\bullet \xrightarrow{k_t} NRP \tag{5}$$

While initiation, propagation and termination reactions are delineated as three distinct elementary steps (Farhoosh, 2021), they occur simultaneously, each possessing its own rate constant. To define the peroxidation rate (R_{uni}), one must solve a system of differential equations in line with the rate laws of Eqs. (2) to (5). This solution was analytically derived using Eq. (6), provided that the rates for the radical species R• and ROO• are set to zero (Cosgrove et al., 1987).

$$R_{uni} = \frac{-\text{d}[\text{O}_2]_{\text{uni}}}{\text{dt}} = \frac{\text{k}_\text{p}}{\sqrt{2\text{k}_\text{t}}} \bullet [\text{RH}] \bullet \sqrt{\text{R}_\text{i}} \tag{6}$$

Where, [O_2] and [RH] represent the molar concentration, respectively, of oxygen and lipid substrate. From this equation, the ratio $k_p/(2k_t)^{1/2}$ represents the oxidizability index (*O.I.*). The *O.I.* value mainly depends on the degree of unsaturation of fatty acids, with linoleic acid that is 24-fold more oxidizable than oleic acid and thousands-fold faster than saturated fatty acids (Baschieri et al., 2019). Consistently, extra virgin olive oils, which contain about 10% linoleic and 80% oleic acid, generally have a lower *O.I.* compared to sunflower oils, which contain about 60% linoleic acid and 20% oleic acid (Borghi et al., 2020).

Antioxidants act as chain-breakers, inhibiting peroxidation by reacting with peroxyl radicals (Eqs. (7) and (8)):

$$Inhibition: \ ROO\bullet + AH \xrightarrow{k_{inh}} ROOH + A\bullet \tag{7}$$

$$ROO\bullet + A\bullet \xrightarrow{k_A} NRP \tag{8}$$

The rate limiting step is the reaction between ROO• and AH (Eq. (7)), while the recombination of the A• and ROO• radicals to afford non-radical products (NRP) is usually very fast (Eq. (8)) and accounts for the typical stoichiometry ($n = 2$) of phenolic antioxidants. The equation expressing the rate of inhibited peroxidation is reported in Eq. (9):

$$R_{inh} = \frac{-\text{d}[\text{O}_2]_{\text{inh}}}{\text{dt}} = \frac{\text{k}_\text{p}}{\text{k}_{\text{inh}}} \bullet \frac{[\text{RH}]_0 \bullet \text{R}_\text{i}}{\text{n} \bullet [\text{AH}]} \tag{9}$$

Here, k_{inh} represents the rate constants of the inhibition step. The ratio k_{inh}/k_p represents the antioxidant efficiency (*A.E.*), reflecting the competition between Eqs. (7) and (4). The *A.E.* expresses the antioxidant activity relative to the rate constant for chain propagation. A higher ratio signifies greater efficiency of the antioxidant compared to the substrate (Apak, 2019).

2.11. Statistical analysis

Calculations and statistical analysis were carried out using XLSTAT (2021.5.1, New York, USA) by applying one-way ANOVA and Fisher's post-hoc test ($p < 0.05$). All the experiments were carried out in duplicates and findings are presented as mean ± standard deviation. Graphics preparation was carried out using graphing and analysis software OriginPro 2021 (9.8.0.200, OriginLab Corporation, USA).

3. Results and discussion

Isothermal Calorimetry was utilized to monitor the real-time autoxidation of mayonnaise samples at 60 °C. Performing the experiments at this temperature accelerates the autoxidation process, thereby making it feasible to measure and monitor within the practical timeframes of our experimental setup. While ambient temperatures (like 20 °C) are relevant for storage, 60 °C mirrors conditions that are more akin to those faced by mayonnaise during certain food processing or cooking steps. Thus, understanding its behaviour at this temperature can have direct relevance to practical applications. A representative calorimetric trace depicting the autoxidation of mayonnaise samples is shown in Fig. 1(A). Initially, the heat flow signal was negligible, signifying the suppression of autoxidation in the mayonnaise due to antioxidants. However, after a few hours, a sudden raise in exothermic heat signified the onset time of lipid autoxidation. Such time is defined the induction period (τ). Its occurrence unequivocally indicates the moment when all the antioxidants present in the sample have been depleted by radicals.

Following the induction period, the oxidation process proceeded uninhibited. Subsequently, the signal reached its peak and then declined steadily to values near zero, indicating the end of the autoxidation process. Interestingly, the trend observed in the IC response and the O_2 consumption measured through the oximetry-based approach showed remarkable similarity. This finding can be elucidated by noting that while every event in lipid peroxidation contributes to the heat absorbed or released by IC, only reactions during the propagation phases (reactions (3) and (4) have a pronounced effect. This is due to their cyclical nature and enhanced substrate conversion for each radical produced by AIBN. Although the antioxidant's reaction with ROO• can produce heat, the minimal heat flow observed at the start of the reaction can be attributed to the antioxidant's inhibition of propagation, therby preventing the emergence of several cycles of the radical chain.

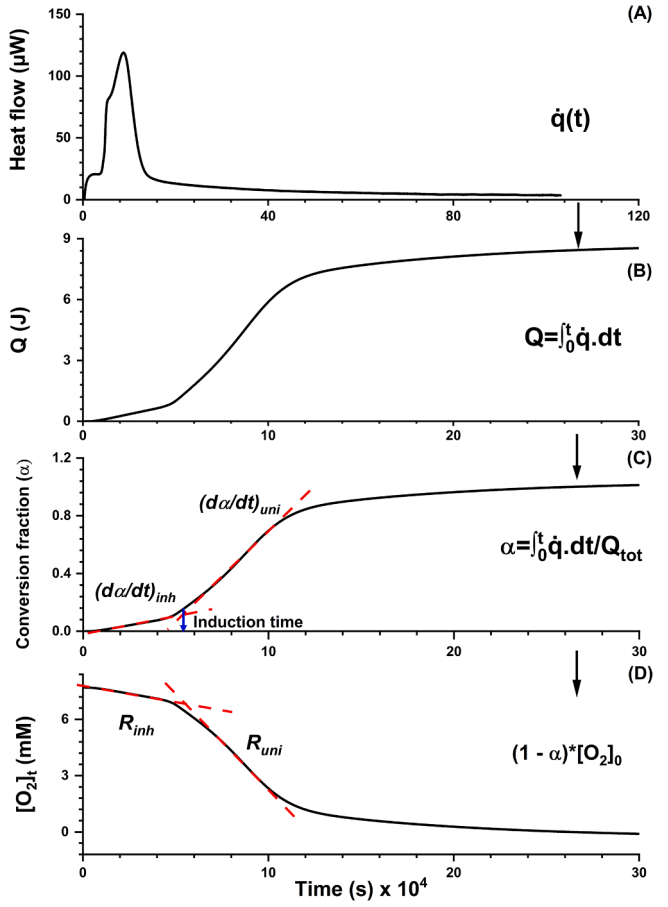

Fig. 1. Schematic representation of the kinetic modelling process (A) isothermal calorimetric heat flow curve; (B) derived heat vs time curve; (C) conversion fraction vs time curve and (D) rate of oxygen consumption.

Considering that in the sample the initial oxygen amount ($O_2 - n = 0.21P/RT = 2.9\times10^{-5}$ mol) was about 22 times smaller than the initial concentration of oxidizable fatty acids (RH_0 ~6.3×10^{-4} mol), oxygen was rate-limiting.

Conversely, the autoxidation process was not limited by the consumption of AIBN. At 60 °C, the thermal decomposition of AIBN proceeded at a rate of initiation, $R_i = 4.4\pm0.1\times10^{-9}$ M/s, as determined by a modified version of the induction period method (Mosibo et al., 2022) (Eq. (10)).

$$R_i = \frac{n \times [\alpha - TOH]}{\tau_f - \tau_c} \quad (10)$$

Where [α −TOH] is the concentration of α-tocopherol (20 μM) that was added to the mayonnaise samples (Supplementary Fig. S1) (Amorati et al., 2016). Finally, τ_f and τ_c are, respectively, the observed induction times for the fortified and non-fortified mayonnaise samples. This approach with fortified samples is ideal because it accounts for the matrix effects of complex samples, such as mayonnaise. R_i was approximately the same in all the mayonnaise samples, indicating that the initiation of the peroxidation is only due to AIBN decomposition. Based on such R_i value and a reaction time of 250 h, no>16% of the initial concentration of AIBN was consumed during the experimental time window.

Next, the calorimetric trace was transformed into oxygen consumption. Fig. 1(B – D) exemplifies the steps needed to transform the heat flow signals into oxygen concentrations. In details, Fig. 1(B) shows the cumulative heat ($q(t)$, in Joule), obtained by integrating the heat flow data (Eq. (11)):

$$q(t) = \int_0^t \phi \bullet dt \quad (11)$$

The plateau value observed when the autoxidation process was left to react for the whole of its lifetime provided the total amount of heat (Q_{tot} ~9 J). As oxygen was the rate-limiting factor, this value corresponded to the total energy generated during the complete consumption of oxygen (2.9×10^{-5} mol) in the ampoule (3.75 cm^3), leading to an average heat of ~300 kJ per mole of oxygen consumed at 60 °C.

Next, from the cumulative heat curve, it was possible to derive the transient conversion fraction of the autoxidation process. This was obtained as the ratio between $q(t)$ and Q_{tot}, as shown in Fig. 1(C). The conversion fraction ($\alpha(t)$) represents the extent of reactant conversion into products, with a value varying from 0 to 1 over time.

Thus, based on the $\alpha(t)$ values, it was straightforward to derive the total concentration of oxygen consumed from Eq. (12):

$$[O_2]_t = \left(\frac{V_H}{V_S}\right) \times \frac{P_{O_2}}{R \bullet T} \times [1 - \alpha(t)] \quad (12)$$

Where V_H (volume of headspace) = 3.75 cm^3, V_S (volume of sample) = 0.25 cm^3, P_{O2} = 0.21 atm, T = 333 K and R = 0.082 L atm/K mol. However, as the autoxidation takes place in the lipid phase, the rate of O_2 consumption to be used in eqs. (6) and (9) must be referred with respect to the volume of the mayonnaise sample, which is 0.25 mL (Eq. (12)). Fig. 1 (D) shows the resulting plot of oxygen consumption over time. From this plot, two tangent lines were drawn, representing, respectively, the rates of oxygen consumption during the inhibited (R_{inh}) and uninhibited (R_{uni}) periods.

Finally, the oxygen concentration values obtained from the isothermal calorimetry curves were compared with those determined by oximetry. Fig. 2 shows the excellent correlation between the two methods for a mayonnaise sample (MCO) prepared with corn oil. Similar results were also obtained with the other four mayonnaise samples, each prepared with different source of vegetable oils (sunflower, extra virgin

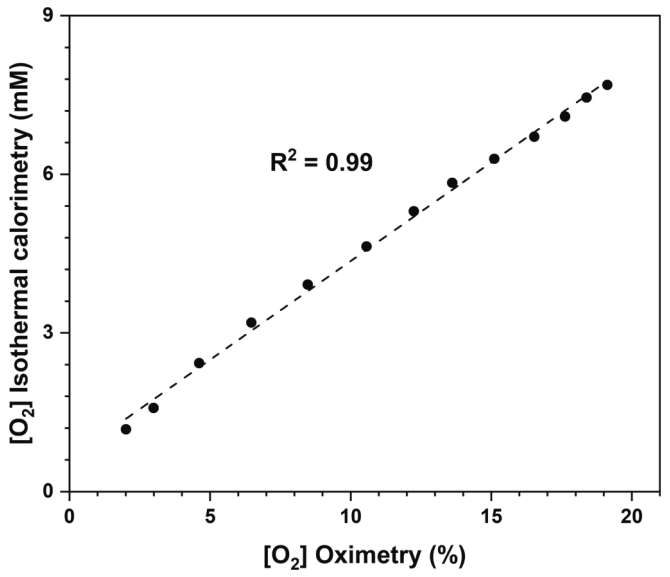

Fig. 2. Correlation between oxygen consumption from oximetry and derived from isothermal calorimetry for MCO.

olive, grapeseed, and apple seed). In all cases, a very high correlations were achieved ($R^2 = 0.99$) (Supplementary Fig. S2). Overall, these results validate the appropriatenessof the proposed calorimetric method for measuring oxygen concentration.

3.1. Oxidizability of mayonnaise

Fig. 3(A) shows the calorimetric traces derived from the analysis of five distinct mayonnaise samples. While each sample was prepared using the same water phase, they utilized different plant-based oils. To ensure droplet size had minimal impact on the oxidizability of mayonnaise, all samples were carefully homogenized until the resulting oil droplets reached an average hydrodynamic radius of about 1–10 μm (as shown in Supplementary Fig. S3). Additionally, due to the high surface area of the resulting oil droplets in the emulsion, slight variations in droplet size did not significantly affect the rate of lipid peroxidation (Waraho et al., 2011).

Fig. 3(B) shows the transformation of the calorimetric trace into the corresponding oxygen consumptions data (vide supra). As previously shown, Fig. 3(B) allowed for the determination of the induction time (τ) for the oxidation of each mayonnaise sample, as well as the rates of oxygen consumption during the inhibited (R_{inh}) and uninhibited (R_{uni}) periods. The results are reported in Table 1. While all samples had comparable initial peroxide values (PV <5 meq O_2/Kg of sample), each sample exhibited unique R_{uni} and R_{inh} values. Previous studies investigating emulsion systems using NMR spectroscopy to determine oxidation products (Boerkamp et al., 2022), observed a decrease in peroxide levels as oxidation progressed. However, the sum of oxidation products (hydroperoxides, epoxides, and aldehydes) correlated well with the total oxygen consumption, particularly during the early oxidation phase (Boerkamp et al., 2022). These results highlight the constraints of solely determining PV and underscore the usefulness of measuring O_2 consumption, either directly or via our IC method. Consequently, PV measurements become less relevant when studying the advanced autoxidation stages of emulsion systems, especially when hydroperoxide decomposition prevails. Also, PV measurements suffers from the presence of water in emulsified systems, as the recovery of peroxides may be complicated by their partition through the two phases (M. Laguerre et al., 2007).

Also, given $[RH]_0$ (Supplementary Table S3) and R_i (see Eq. (10)), the measurement of R_{uni} leads to the oxidizability index (*O.I.*) of the mayonnaise samples based on Eq. (13).

Table 1
Kinetic parameters derived using the isothermal calorimetry trace of mayonnaise samples at 60 °C.

Sample	R_{inh} 10^{-7} mol/L.s	R_{uni} 10^{-7} mol/L.s	*O.I.* 10^{-3} $(mol/L)^{-1/2}s^{-1/2}$	k_p $(mol/L)^{-1}s^{-1}$	τ 10^4 s	*A.E.* -	k_{inh} 10^3 $(mol/L)^{-1}s^{-1}$
MSO	2.3 ±0.1^c	14.2 ±1.1^a	8.7 ±0.6^a	29.0 ±1.9^a	5.4 ±0.1^d	198.1 ±6.6^a	5.7 ±0.2^a
MCO	2.8 ±0.1^b	5.2 ±0.2^c	3.2 ±0.1^c	11.0 ±0.1^c	11.8 ±0.9^b	74.8 ±4.4^d	0.8 ±0.1^d
MEVOO	1.6 ±0.1^d	2.5 ±0.1^d	1.7 ±0.1^d	5.7 ±0.1^d	18.8 ±0.4^a	77.4 ±2.9^d	0.4 ±0.1^d
MGO	2.9 ±0.1^b	8.8 ±1.5^b	5.4 ±0.9^b	18.3 ±2.8^b	7.8 ±0.1^c	108.0 ±4.6^c	2.0 ±0.1^c
MAO	4.1 ±0.3^a	14.8 ±0.2^a	8.9 ±0.1^a	30.0 ±0.5^a	4.8 ±0.2^d	128.6 ±10.5^b	3.9 ±0.3^b

R_{inh}: rate of oxidation during inhibited period; R_{uni}: rate of oxidation during uninhibited period; O.I.: oxidizability index; k_p: propagation rate constant; τ: induction period, A.E.: antioxidant efficiency and k_{inh}: inhibition rate constant. In a column means ± SD that do not share a superscript letter are significantly different ($p < 0.05$).

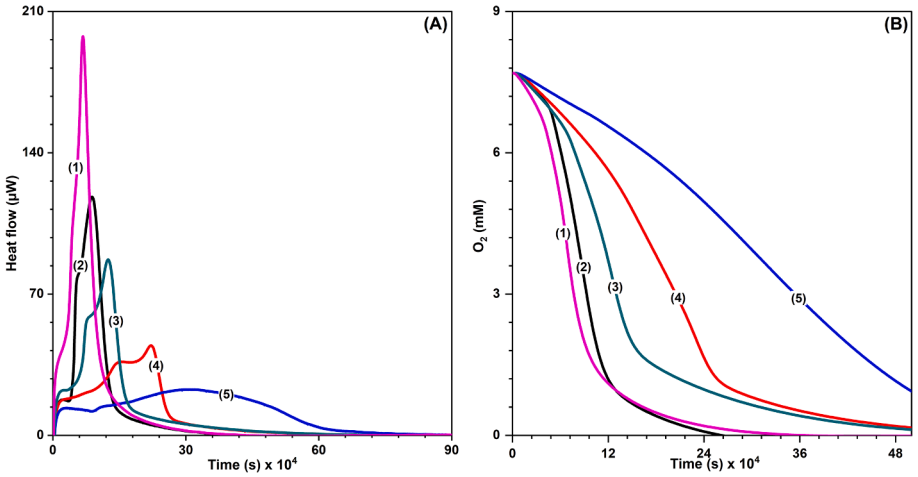

Fig. 3. (A) Isothermal calorimetry trace of mayonnaise at 60 °C, (B) oxygen consumption derived from heat flow data. (1) MAO, (2) MSO, (3) MGO, (4) MCO and (5) MEVOO.

$$O.I. = \frac{k_p}{\sqrt{2k_t}} = \frac{R_{uni}}{[RH]_0 \bullet \sqrt{R_i}} \quad (13)$$

Table 1 reports the resulting *O.I.* values. In details, the mayonnaise samples with the highest *O.I.*, indicating the highest susceptibility to oxidation, are those made from apple seed oil and sunflower oil. There is no statistical significant difference ($p > 0.05$) between them. They are followed by grape seed oil > corn oil > extra virgin olive oil. The *O.I.* values strongly correlate with the content of unsaturated fatty acids ($R^2 = 0.99$). This correlation is expected considering that the rate constant for a termination reaction, $2k_t$, remains consistent among different oxidizable substrates ($\sim 10^7\ M^{-1}s^{-1}$) (Baschieri et al., 2019). In contrast, the values for the propagation rate constant, k_p, greatly depend on the degree of unsaturation in the fatty acids (Xu et al., 2009). Moreover, the k_p values, which can be derived from *O.I.*, and a $2k_t$ value of $10^7\ M^{-1}s^{-1}$ are of the same order of magnitude (Table 1) as those determined in homogeneous system by oximetry technique, where the k_p of pure methyl linoleate is 62 $M^{-1}s^{-1}$.

3.2. Antioxidant efficiency

The concept of "antioxidant efficiency" provides a beneficial and practical approach to quantitatively describe the effects of antioxidants in inhibiting lipid peroxidation (Bravo-Díaz, 2022). The *A.E.* of mayonnaise samples is given by Eq. (14) (Pryor et al., 1993). Since R_i remains constant across all the mayonnaise samples, *A.E.* can be simply expressed using the onset time (τ) and R_{inh}.

$$A.E. = \frac{k_{inh}}{k_p} = \frac{R_i}{n \bullet [AH]_0} \bullet \frac{[RH]_0}{R_{inh}} = \frac{[RH]_0}{\tau \bullet R_{inh}} \quad (14)$$

Based on the results reported in Table 1, the mayonnaise made with sunflower oil showed the highest *A.E.* value. This was followed by apple seed oil > grapeseed oil > extra virgin olive oil & corn oil. Notably, there was no significant difference ($p > 0.05$) between extra virgin olive oil and corn oil. The *A.E.* of sunflower oil-based mayonnaise was approximately 2.5 times higher than in the mayonnaises made with extra virgin olive oil and corn oil, and 1.8 and 1.5 times higher than those made with grapeseed and apple seed oils, respectively. This is explained by the greater reactivity of the antioxidants in sunflower oil towards neutralizing free radicals, as reflected by the higher k_{inh} (Table 1). Furthermore, since the concentration of antioxidant is typically much lower than that of the oxidizable substrate, the k_{inh} value is expected to be much higher than k_p ($k_{inh} \gg k_p$) (Barclay et al., 1999). The k_{inh} values determined for the antioxidants present in these oils align with the range reported by Baschieri et al., (2019) for typical antioxidants in essential oils. Although extra virgin olive oil contains the highest concentration of antioxidants, as determined by DPPH, ORAC, TPC (Table 2), its relatively lower *A.E.* is likely because, in our model system, peroxyl radicals are generated in the lipid phase due to the thermal degradation of AIBN. Thus, oils rich in lipid soluble antioxidants, like tocopherols, have a higher *A.E.* index since these antioxidants are located where radicals form. Conversely, extra virgin olive oil is especially rich in polar phenolics, such as oleuropein and hydroxytyrosol (Edwin N. Frankel, 2010), which are more effective in the water phase and, therefore, far from the peroxyl radicals. In agreement with the partitioning effect explained by Bravo-Díaz, (2022), the antioxidants need to be properly positioned where the radicals are produced to protect the unsaturated lipids. In other words, an antioxidant must be in the right place at the right time (Mickaël Laguerre et al., 2015).

Nevertheless, given the low oxidative index (*O.I.*) of MEVOO (see Table 1), overall, mayonnaise samples prepared with extra virgin olive oil was the most stable against peroxidation.

4. Conclusion

In this study, isothermal calorimetry was applied for the first time to simultaneously determine the antioxidant activity, capacity, and oxidizability of mayonnaise samples. The high sensitivity of the heat flow sensors, combined with the unmatched long-term thermal stability of the apparatus, made these results possible. Furthermore, the unique feature to measure emulsions in a solvent-free environment, without the need for sample preparation (i.e., without breaking the emulsion), was pivotal in obtaining these results. Overall, isothermal calorimetry emerges as an efficient and reliable technique for the rapid screening of a wide range of complex lipid systems. It is noteworthy that this study focused on assessing the antioxidant efficiency and oxidizability of mayonnaise by initiating autoxidation in the lipid phase. Future research will explore the effects of initiating autoxidation in the aqueous phase.

Table 2
Antioxidant assays and total phenolic content of oils.

Sample	DPPH	ORAC	TPC
	mmol TE/L	mmol TE/L	mmol GAE/L
Sunflower oil	2.57 ± 0.06^{d}	2.41 ± 0.32^{c}	3.04 ± 0.19^{d}
Corn oil	3.46 ± 0.13^{b}	3.65 ± 0.23^{b}	3.35 ± 0.10^{b}
Extra virgin olive oil	4.49 ± 0.09^{a}	6.20 ± 0.50^{a}	4.12 ± 0.06^{a}
Grapeseed oil	3.14 ± 0.15^{c}	3.81 ± 0.48^{b}	3.24 ± 0.05^{bc}
Apple seed oil	2.31 ± 0.06^{e}	3.23 ± 0.42^{b}	3.06 ± 0.06^{cd}

DPPH: DPPH antioxidant assay; ORAC: oxygen radical absorbance capacity; TPC: total phenolic content; TE: Trolox equivalent; GAE: gallic acid equivalent. In a column means ± SD that do not share a superscript letter are significantly different ($p < 0.05$).

CRediT authorship contribution statement

Rajat Suhag: Conceptualization, Methodology, Formal analysis, Investigation, Data curation, Writing – original draft. **Giovanna Ferrentino:** Formal analysis, Investigation, Data curation. **Ksenia Morozova:** Formal analysis, Investigation, Data curation. **Daniele Zatelli:** Resources. **Matteo Scampicchio:** Conceptualization, Methodology, Writing – review & editing, Project administration, Supervision. **Riccardo Amorati:** Writing – review & editing.

Declaration of Competing Interest

The authors declare the following financial interests/personal relationships which may be considered as potential competing interests: Matteo Scampicchio reports financial support was provided by Italian Ministry of University and Research.

Data availability

Data will be made available on request.

Acknowledgements

Award Number: Project code PE00000003, Concession Decree No. 1550 of 11 October 2022 adopted by the Italian Ministry of University and Research, CUP D93C22000890001, Project title "ON Foods – Research and innovation network on food and nutrition Sustainability, Safety and Security – Working ON Foods".

Project funded under the National Recovery and Resilience Plan (NRRP), Mission 4 Component 2 Investment 1.3 – Call for tender No. 341 of 15 March 2022 of Italian Ministry of University and Research funded by the European Union – NextGenerationEU;

Appendix A. Supplementary data

Supplementary data to this article can be found online at https://doi.org/10.1016/j.foodchem.2023.137274.

References

Amorati, R., Baschieri, A., Morroni, G., Gambino, R., & Valgimigli, L. (2016). Peroxyl Radical Reactions in Water Solution: A Gym for Proton-Coupled Electron-Transfer Theories. *Chemistry - A European Journal, 22*(23), 7924–7934. https://doi.org/10.1002/chem.201504492

Amorati, R., & Valgimigli, L. (2015). Advantages and limitations of common testing methods for antioxidants. *Free Radical Research, 49*(5), 633–649. https://doi.org/10.3109/10715762.2014.996146

Amorati, R., & Valgimigli, L. (2018). Methods To Measure the Antioxidant Activity of Phytochemicals and Plant Extracts. *Journal of Agricultural and Food Chemistry, 66*(13), 3324–3329. https://doi.org/10.1021/acs.jafc.8b01079

Apak, R. (2019). Current Issues in Antioxidant Measurement. *Journal of Agricultural and Food Chemistry, 67*(33), 9187–9202. https://doi.org/10.1021/acs.jafc.9b03657

Barclay, L. R. C., Edwards, C. E., & Vinqvist, M. R. (1999). Media effects of antioxidant activities of phenols and catechols. *Journal of the American Chemical Society, 121*(26), 6226–6231. https://doi.org/10.1021/ja990878u

Baschieri, A., & Amorati, R. (2021). Methods to Determine Chain-Breaking Antioxidant Activity of Nanomaterials beyond DPPH•. *A Review. Antioxidants, 10*(10), 1551. https://doi.org/10.3390/antiox10101551

Baschieri, A., Pizzol, R., Guo, Y., Amorati, R., & Valgimigli, L. (2019). Calibration of Squalene, p -Cymene, and Sunflower Oil as Standard Oxidizable Substrates for Quantitative Antioxidant Testing. *Journal of Agricultural and Food Chemistry, 67*(24), 6902–6910. https://doi.org/10.1021/acs.jafc.9b01400

Berton-Carabin, C. C., Ropers, M.-H., & Genot, C. (2014). Lipid Oxidation in Oil-in-Water Emulsions: Involvement of the Interfacial Layer. *Comprehensive Reviews in Food Science and Food Safety, 13*(5), 945–977. https://doi.org/10.1111/1541-4337.12097

Boerkamp, V. J. P., Merkx, D. W. H., Wang, J., Vincken, J. P., Hennebelle, M., & van Duynhoven, J. P. M. (2022). Quantitative assessment of epoxide formation in oil and mayonnaise by 1H–13C HSQC NMR spectroscopy. *Food Chemistry, 390*, Article 133145. https://doi.org/10.1016/j.foodchem.2022.133145

Borghi, F. T., Santos, P. C., Santos, F. D., Nascimento, M. H. C., Corrêa, T., Cesconetto, M., … Filgueiras, P. R. (2020). Quantification and classification of vegetable oils in extra virgin olive oil samples using a portable near-infrared spectrometer associated with chemometrics. *Microchemical Journal, 159*, Article 105544. https://doi.org/10.1016/j.microc.2020.105544

Brand-Williams, W., Cuvelier, M. E., & Berset, C. (1995). Use of a free radical method to evaluate antioxidant activity. *LWT - Food Science and Technology, 28*(1), 25–30. https://doi.org/10.1016/S0023-6438(95)80008-5

Bravo-Díaz, C. (2022). Advances in the control of lipid peroxidation in oil-in-water emulsions: Kinetic approaches†. *Critical Reviews in Food Science and Nutrition, 1–33*. https://doi.org/10.1080/10408398.2022.2029827

Carocho, M., Morales, P., & Ferreira, I. C. F. R. (2018). Antioxidants: Reviewing the chemistry, food applications, legislation and role as preservatives. *In Trends in Food Science and Technology, 71*, 107–120. https://doi.org/10.1016/j.tifs.2017.11.008

Cosgrove, J. P., Church, D. F., & Pryor, W. A. (1987). The kinetics of the autoxidation of polyunsaturated fatty acids. *Lipids, 22*(5), 299–304. https://doi.org/10.1007/BF02533996

Culler, M. D., Bayram, I., & Decker, E. A. (2022). Enzymatic Modification of Lecithin for Improved Antioxidant Activity in Combination with Tocopherol in Emulsions and Bulk Oil. *Journal of Agricultural and Food Chemistry, 70*(41), 13404–13412. https://doi.org/10.1021/acs.jafc.2c05182

Domínguez, R., Pateiro, M., Gagaoua, M., Barba, F. J., Zhang, W., & Lorenzo, J. M. (2019). A Comprehensive Review on Lipid Oxidation in Meat and Meat Products. *Antioxidants, 8*(10), 429. https://doi.org/10.3390/antiox8100429

Farhoosh, R. (2021). Initiation and propagation kinetics of inhibited lipid peroxidation. *Scientific Reports, 11*(1), 6864. https://doi.org/10.1038/s41598-021-86341-9

Ferrentino, G., Giampiccolo, S., Morozova, K., Haman, N., Spilimbergo, S., & Scampicchio, M. (2020). Supercritical fluid extraction of oils from apple seeds: Process optimization, chemical characterization and comparison with a conventional solvent extraction. *Innovative Food Science & Emerging Technologies, 64*, Article 102428. https://doi.org/10.1016/j.ifset.2020.102428

Frankel, E. N., Hu, M. L., & Tappel, A. L. (1989). Rapid headspace gas chromatography of hexanal as a measure of lipid peroxidation in biological samples. *Lipids, 24*(11), 976–981. https://doi.org/10.1007/BF02544544

Frankel, E. N. (2010). Chemistry of extra virgin olive oil: Adulteration, oxidative stability, and antioxidants. *Journal of Agricultural and Food Chemistry, 58*(10), 5991–6006. https://doi.org/10.1021/jf1007677

Frankel, Edwin N. (2012). Hydroperoxide decomposition. In E. N. B. T.-L. O. (Second E. Frankel (Ed.), Lipid Oxidation (pp. 67–98). Elsevier. https://doi.org/10.1533/9780857097927.67.

ten Klooster, S., Schroën, K., & Berton-Carabin, C. (2023). Lipid oxidation products in model food emulsions: Do they stay in or leave droplets, that's the question. *Food Chemistry, 405*, Article 134992. https://doi.org/10.1016/j.foodchem.2022.134992

Koelsch, C. M., Downes, T. W., & Labuza, T. P. (1991). Hexanal Formation via Lipid Oxidation as a Function of Oxygen Concentration: Measurement and Kinetics. *Journal of Food Science, 56*(3), 816–820. https://doi.org/10.1111/j.1365-2621.1991.tb05389.x

Laguerre, M., Lecomte, J., & Villeneuve, P. (2007). Evaluation of the ability of antioxidants to counteract lipid oxidation: Existing methods, new trends and challenges. *Progress in Lipid Research, 46*(5), 244–282. https://doi.org/10.1016/j.plipres.2007.05.002

Laguerre, M., Bayrasy, C., Panya, A., Weiss, J., McClements, D. J., Lecomte, J., … Villeneuve, P. (2015). What Makes Good Antioxidants in Lipid-Based Systems? The Next Theories Beyond the Polar Paradox. *Critical Reviews in Food Science and Nutrition, 55*(2), 183–201. https://doi.org/10.1080/10408398.2011.650335

Mosibo, O. K., Scampicchio, M., & Ferrentino, G. (2022). Calorimetric adaptation of the inhibited autoxidation method to determine the activity of individual antioxidants and natural extracts. *Journal of Thermal Analysis and Calorimetry, 147*(22), 12829–12836. https://doi.org/10.1007/s10973-022-11399-0

Ou, B., Hampsch-Woodill, M., & Prior, R. L. (2001). Development and Validation of an Improved Oxygen Radical Absorbance Capacity Assay Using Fluorescein as the Fluorescent Probe. *Journal of Agricultural and Food Chemistry, 49*(10), 4619–4626. https://doi.org/10.1021/jf010586o

Pryor, W. A., Cornicelli, J. A., Devall, L. J., Tait, B., Trivedi, B. K., Witiak, D. T., & Wu, M. (1993). A rapid screening test to determine the antioxidant potencies of natural and synthetic antioxidants. *The Journal of Organic Chemistry, 58*(13), 3521–3532. https://doi.org/10.1021/jo00065a013

Schröder, A., Sprakel, J., Boerkamp, W., Schroën, K., & Berton-Carabin, C. C. (2019). Can we prevent lipid oxidation in emulsions by using fat-based Pickering particles? *Food Research International, 120*, 352–363. https://doi.org/10.1016/j.foodres.2019.03.004

Sicari, M., Stevanato, R., Ongaro, I., Zuliani, R., Ravagnan, G., & Lucchini, V. (2018). Searching for an absolute kinetic scale of antioxidant activity against lipid peroxidation. *Food Chemistry, 239*, 964–974. https://doi.org/10.1016/j.foodchem.2017.06.139

Tinello, F., Lante, A., Bernardi, M., Cappiello, F., Galgano, F., Caruso, M. C., & Favati, F. (2018). Comparison of OXITEST and RANCIMAT methods to evaluate the oxidative stability in frying oils. *European Food Research and Technology, 244*(4), 747–755. https://doi.org/10.1007/s00217-017-2995-y

Valoppi, F., Haman, N., Ferrentino, G., & Scampicchio, M. (2020). Inhibition of lipid autoxidation by vegetable waxes. *Food & Function, 11*(7), 6215–6225. https://doi.org/10.1039/D0FO01022G

Villeneuve, P., Bourlieu-Lacanal, C., Durand, E., Lecomte, J., McClements, D. J., & Decker, E. A. (2023). Lipid oxidation in emulsions and bulk oils: A review of the importance of micelles. *Critical Reviews in Food Science and Nutrition, 63*(20), 4687–4727. https://doi.org/10.1080/10408398.2021.2006138

Wang, D., Xiao, H., Lyu, X., Chen, H., & Wei, F. (2023). Lipid oxidation in food science and nutritional health: A comprehensive review. *Oil Crop Science, 8*(1), 35–44. https://doi.org/10.1016/j.ocsci.2023.02.002

Waraho, T., McClements, D. J., & Decker, E. A. (2011). Mechanisms of lipid oxidation in food dispersions. *Trends in Food Science & Technology, 22*(1), 3–13. https://doi.org/10.1016/j.tifs.2010.11.003

Xu, L., Davis, T. A., & Porter, N. A. (2009). Rate Constants for Peroxidation of Polyunsaturated Fatty Acids and Sterols in Solution and in Liposomes. *Journal of the American Chemical Society, 131*(36), 13037–13044. https://doi.org/10.1021/ja9029076

Yildirim, M., Sumnu, G., & Sahin, S. (2016). Rheology, particle-size distribution, and stability of low-fat mayonnaise produced via double emulsions. *Food Science and Biotechnology, 25*(6), 1613–1618. https://doi.org/10.1007/s10068-016-0248-7